

Testing the local density approximation with energy-versus-separation curves of jellium slab pairs

John F. Dobson and Jun Wang

School of Science, Griffith University, Nathan, Queensland 4111, Australia

(Received 28 May 2003; revised manuscript received 11 December 2003; published 9 June 2004)

We explore the successes and failures of the local-density approximation (LDA) in predicting the attractive force and energetics of attraction between two jellium metals. We model the metals by two very thin slabs, and follow the energetics at all separations D from the van der Waals (vdW) regime at large D through to metallic bonding as $D \rightarrow 0$. We compare LDA results with calculations including exact exchange and microscopic nonlocal random-phase-approximation-type correlation energy: only these latter calculations include dispersion (van der Waals) forces correctly. We show how this error of LDA at large separations leads also to errors even at smaller separations outside the vdW regime.

DOI: 10.1103/PhysRevB.69.235104

PACS number(s): 71.15.Mb, 71.10.Ca, 73.61.At

I. INTRODUCTION

Ground-state electronic density-functional theory¹ has been a mainstay of condensed matter theory for many years. In its local form [local-density approximation² (LDA)] and in various types of generalized gradient approximation (GGA, e.g., Ref. 3), it has provided many-electron ground-state energies of a wide range of systems, with sufficient accuracy to permit practical prediction of structural properties. Currently, there is growing interest in the structural energetics of soft condensed matter, with applications ranging from a clean energy economy (via hydrogen storage in graphenes) through polymer properties to possible issues in biological systems. In these soft systems the weak dispersion or van der Waals (vdW) forces are often believed to be important. Here the LDA/GGA potentially run into problems because it is known that these approximations completely miss the dispersion interaction between distant systems whose electronic densities do not overlap (see, e.g., Ref. 4). The situation is less clear where electron clouds overlap. For example, there is a school of thought that models interactions of graphitic systems using vdW force models.⁵ On the other hand, another school finds that the LDA is good for graphitic systems near equilibrium geometry, regardless of the possible presence of vdW interactions.⁶ [The same is not true for the GGA (Refs. 7 and 8), for reasons that are at least partly understood.⁹] A resolution of this issue regarding use of the LDA for soft layered systems is clearly important, if the current development of soft-matter physics is to progress optimally.

In this connection, an archetypal problem is the energetics of a pair of infinite parallel graphene planes as a function of their separation distance D . This problem has recently been examined using nonlocal random-phase-approximation (RPA)-like formalism, but in a highly approximate form.⁷ Unfortunately this problem appears to be too delicate for this approximate approach, as different approximations within the same framework^{7,8} gave significantly different binding energies. It therefore seems that an unequivocal resolution of the LDA issue will require nonlocal correlation theories to be evaluated numerically without approximation, at least for a

few benchmark cases. This appears to be barely within reach of current computational technology, and is presently underway in more than one group, for the case of graphene planes and bulk graphite. Initial numbers appear to confirm the delicacy of the problem.

The present paper contributes to this field by using a simpler system that has some similarity to a pair of graphene planes, but that is much more easily solvable numerically. Specifically, we treat a pair of parallel nearly two-dimensional (2D) jellium metal slabs. Such problems with one-dimensional spatial inhomogeneity have recently become amenable to analysis via microscopic nonlocal correlation theories.¹⁰⁻¹³ Our thin jellium slabs share an essential feature with a pair of graphene planes, namely an extreme anisotropy of the electronic response parallel and perpendicular to the layers. In the case of our jellium slabs, the response is free-electron-like parallel to the planes—i.e., we have a pair of nearly 2D metals. The isolated graphene layers are *zero-gap* insulators in the plane, again with extreme anisotropy, and they become highly anisotropic weak metals in the overlapped configuration of bulk graphite. For our simpler system we will show that the failure of the LDA to obtain the vdW energy at large separations D also has repercussions for its performance near to the equilibrium separation. While this cannot simply be taken across to the graphitic problem, it certainly sheds significant doubt on the validity of LDA for layered systems such as stretched graphite.

The present work also touches on another current controversy, concerning the surface energy of simple metals. The LDA provided the first reasonably realistic first-principles predictions¹⁴ of simple-metal surface or cleavage energies σ . The initial step in these predictions was a calculation for the jellium or electron-gas model in which the discrete ions are replaced by a uniform positive background. The jellium surface energy $\sigma(r_s)$ is a fundamental property of the electron gas, and continues to attract considerable interest and controversy^{9,15,16} because of the inhomogeneous many-electron exchange and correlation physics that it embodies.

The number density

$$n = \left(\frac{4}{3} \pi r_s^3 a_B^3 \right)^{-1} \quad (1)$$

of the electron gas is traditionally specified in terms of the dimensionless Wigner-Seitz radius r_s and the Bohr radius a_B .

$\sigma(r_s)$ can be obtained in principle from the work $2\sigma(r_s) = -E^{\text{cross}}(r_s, D=0)$ done per unit area, in separating two infinitely thick jellium slabs from contact at $D=0$ (metallic binding) through to infinite separation, $D \rightarrow \infty$. In fact the whole binding curve $E^{\text{cross}}(r_s, D)$ is of interest, giving the variation of the total electronic energy per unit area of two slabs, as a function of the separation D between the near edges of the positive jellium backgrounds. Naturally this curve reflects information about the metallic binding phenomena occurring for the region $D \sim$ a few Angstroms, where the electronic densities overlap. Equally, however, it exhibits van der Waals forces occurring at larger distances for which there is little or no overlap. The former region $D \rightarrow 0$ might be considered a natural case for the LDA because of a relatively slow spatial variation of the density $n(z)$. In the opposite limit, $D \rightarrow \infty$, the vdW force is dominant: the LDA and related GGA's fail to describe this at all. There are relatively simple analyses that can deal adequately with this distant region, however, either via random phase approximation or via a hydrodynamic approximation to the RPA response functions. These approaches agree in predicting an interaction energy proportional to $D^{-5/2}$ for thin slabs and to D^{-2} for thick ones, in the region where overlap is negligible but electromagnetic retardation is not significant.^{4,11,17} The intermediate region is therefore of most interest, and indeed we have recently argued¹¹ that a reliable analysis of this region requires a very nonlocal electron correlation model of the inhomogeneous RPA class, or beyond. Using this approach we showed,¹¹ for the case $r_s=2.07$ and for very thin jellium slabs, that the correlation energy is very poorly given by the LDA at all separations.

The present paper extends this type of analysis to the *total* electronic binding-energy curves and force curves of two very thin jellium slabs at a range of metallic electron number densities. For the RPA and RPA-like calculations, we included exact exchange. For the LDA calculation, local exchange is added to the very poor local correlation energy. As frequently occurs in LDA calculations, we find a near cancellation between the errors in local exchange and local correlation. This yields a relatively good performance for the total energy near the equilibrium separation. We show in the present paper that this holds for a range of r_s values. As is well known, the LDA surface energy is surprisingly good, despite the failure of LDA to obtain any vdW force at large separations. Our results show, however, that the binding force $F(D)$ is often overestimated by LDA at intermediate separations D , then underestimated at large D , resulting in a relatively good contact or surface energy from the integral $\int F(D)dD$.

In fact, given that the LDA misses the distant vdW force, it must necessarily overestimate the force at intermediate distance, in order to achieve the good energy that it sometimes does do, near to the equilibrium separation D_0 . That is, LDA cannot obtain both a good equilibrium energy (related to the surface energy) and a good binding force curve. We will quantify this general argument below, finding that these concerns are indeed significant for thin jellium slabs in the higher range of metallic densities.

II. METHODS

We solve the two-layer jellium problem within a highly nonlocal RPA-like correlation energy theory that treats vdW and other forces seamlessly on an equal footing. Of course the absolute correlation energies for our slab system from the RPA are not particularly good, since in general the RPA treats short-ranged correlations crudely, and typically overestimates correlation energies as a result. This behavior is well known from the uniform electron gas, for example. However, it is now also well known that *differences* in the RPA correlation energy for different inhomogeneous configurations (with the number N of electrons fixed) are typically much better (see, e.g., Ref. 18). One such energy difference is the cross energy (or slab-slab interaction) to be discussed below. In fact for the parallel slab problem at hand, one can show analytically, from a form of the f -sum rule,¹⁹ that the frequencies of the long-wavelength coupled plasmon modes that give rise to the distant vdW interaction are unaffected when one supplements the RPA screening equation with any spatially short-ranged xc kernel f_{xc} . Thus RPA gives the correct plasmon zero point energy for well separated slabs, in accord with the f -sum rule, and this is what creates the vdW energy. In earlier work¹² we added a local energy-optimized xc kernel in the RPA-like screening equation of time-dependent density-functional theory. We verified that this made no difference to the distant vdW interaction between jellium slabs within the adiabatic-connection-fluctuation-dissipation approach, as must be so from the argument just sketched. More importantly, we found that the added xc kernel had essentially no effect on the jellium slab interaction even down to the bonded regime with metallic contact. Thus there is good evidence that the RPA xc energy is essentially perfect for the energy versus separation curves of these thin jellium slabs. Any violation of this conclusion (at large separations at least) would require a long-ranged part of the exchange-correlation kernel f_{xc} relating to motion parallel to the planes. Again, such contributions are known for inhomogeneous systems²⁰⁻²² but seem unlikely here because of the homogeneity parallel to the layers. Thus, except where noted, in what follows we will treat the RPA correlation energy differences as the benchmark for testing more approximate theories.

Our primary aim was to calculate the groundstate energy of two juxtaposed thin jellium slabs as a function of slab separation D , using the nonlocal RPA and related methods. The positive jellium background charge density is of form

$$\rho_+(z) = \begin{cases} 0, & |z| > \frac{1}{2}D + L \\ en_0, & \frac{1}{2}D \leq |z| \leq \frac{1}{2}D + L \\ 0, & |z| < \frac{1}{2}D \end{cases}$$

This represents two parallel slabs of positively charged jellium background, each having thickness L measured in the z direction, with their near edges separated by distance D . The slabs are of infinite extent in the x and y directions. Our system is thus a crude (jellium) model of a pair of very thin juxtaposed metal slabs. A neutralizing amount of fully interacting electron gas is added to this jellium background. We are attempting here to understand the limitations of the LDA, not to model the detailed energetics of real metals. In real metals the energetics of slab separation will depend on details of lattice distortions, and could vary widely between metals of similar electron number density, because of different lattice structures and pseudopotentials. In our jellium model there is no lattice distortion physics, and the energies are smooth functions of electron density across the metallic range. A sampling at $r_s=2.07, 4.0$, and 6.0 therefore suffices.

The steps in our procedure were as follows:

(i) For each slab charge density n_0 parametrized by the Wigner-Seitz radius r_s [Eq. (1)], we used a single fixed slab thickness L . To describe the ground-state electron density $n(z)$, we solved the Kohn-Sham (KS) LDA equations self-consistently for each slab separation D . For the uniform-gas correlation energy $\varepsilon_c(n)$ we used the PW92 (Ref. 23) parametrization, in the slabs with $r_s=4.0$ and $r_s=6.0$. (These were new calculations for the present work.) In the slabs with $r_s=2.07$ we took all data from previous runs.²⁴ In the latter case we had used the Wigner parametrization of $\varepsilon_c(n)$. The ground-state electron-density profile $n(z)$ and Kohn-Sham potential $V_{KS}(z)$ are given in Fig. 1 for $r_s=2.07$ a.u., $L=5.0$ a.u., $D=10.0$ a.u. The KS potentials from the Wigner and PW92 parametrizations are virtually identical, and the densities are not distinguishable at all on the scale of the figure. This suggests that the effect of using different parametrizations of local xc is not significant compared with the effects of nonlocal exchange and correlation to be discussed below.

The electron clouds overlap at small D values, giving a metallic bond. The overlap decreases exponentially at large separations. At very large separations ($D \gg r_s, D \gg L$) there is negligible overlap and we are in the pure vdW attraction regime. Here electron hydrodynamics gives accurate answers for the vdW energy via the zero point energy of coupled two-dimensional plasmons, and agrees with microscopic RPA calculations. (See Refs. 4 and 25.) Thus a detailed microscopic RPA calculation would not be needed if merely this asymptotic regime were under study. We wished to look at intermediate and small separations as well, however, so we needed to perform microscopic response calculations as described below.

(ii) Next, the Kohn-Sham (independent-electron) density-

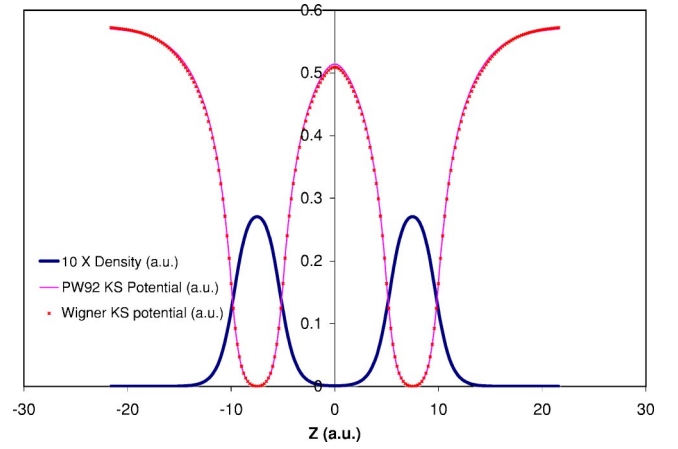


FIG. 1. (Color online) Ground-state electron number density $n(z)$ and Kohn-Sham potential $v_{KS}(z)$ for two neutral jellium slabs each of thickness $L=5$ a.u. with the near edges of the jellium background separated by $D=10$ a.u. Solid lines: Wigner xc used as input to the LDA. Small crosses: PW92 xc used as input to the LDA (for the potential only: in the case of the density plot, the Wigner and PW92 results are not distinguishable on the scale of the diagram).

density response function $\chi_{KS}(\omega=is, q_{\parallel}, z, z')$ was calculated for a range of surface-parallel wave vectors q_{\parallel} and imaginary frequencies $\omega=is$. This is the dynamic density-density response of independent electrons moving in the potential $V_{KS}(z)$. It was obtained as a sum over occupied eigenfunctions $\phi_j(z)$ and eigenvalues ε_j of the KS potential $V_{KS}(z)$:²⁶

$$\chi_{KS}(\omega=is, q_{\parallel}, z, z') = \frac{-2m}{\pi^2 \hbar^2} \sum_{j \text{ occ}} \phi_j(z) \phi_j(z') \int_{-k_j}^{k_j} dk_x \sqrt{k_j^2 - k_z^2} \times \left\{ \frac{\psi^R(\varepsilon^+, z_{>}) \psi^L(\varepsilon^+, z_{<})}{W(\varepsilon^+)} + [\varepsilon^+ \rightarrow \varepsilon^-] \right\}. \quad (2)$$

Here $k_j^2 = 2m(\mu - \varepsilon_j) / \hbar^2$, while $z_{>}$ ($z_{<}$) is the greater (lesser) of z and z' . The complex energies in Eq. (2) are

$$\varepsilon^{\pm} = \pm \hbar is + \varepsilon_j + \frac{\hbar^2}{2m} (2k_x q_{\parallel} - q_{\parallel}^2).$$

The right and left solutions ψ^R, ψ^L arise from construction of the one-dimensional one-particle Green function. They obey the Schrodinger equation with potential V_{KS} at complex energy $\varepsilon = \varepsilon^{\pm}$, with boundary conditions $\psi^{R(L)} \rightarrow 0$ as $z \rightarrow \infty(-\infty)$. Their Wronskian

$$W(\varepsilon) = \psi^R \frac{d\psi^L}{dz} - \psi^L \frac{d\psi^R}{dz}$$

is independent of z , as can be verified from the fact that ψ^R and ψ^L are Schrodinger solutions at the same energy ε .

(iii) The RPA or RPA-like interacting response was calculated by solving the Dyson-like screening integral equation²⁷

$$\chi_\lambda = \chi_{KS} + \chi_{KS} * (\lambda U + f_{xc\lambda}) * \chi_\lambda, \quad (3)$$

where the star represents convolution in the space variable z . In the present geometry (3) becomes a one-dimensional integral equation which can be solved for the interacting response χ_λ :

$$\int_{-\infty}^{\infty} \varepsilon(z, z'') \chi_\lambda(q_\parallel, z'', z', \omega = is) dz'' = \chi_0(q_\parallel, z, z', \omega = is). \quad (4)$$

Here

$$\varepsilon = I - (V_{coul} + f_{xc}) * \chi_0, \quad (5)$$

i.e.,

$$\begin{aligned} \varepsilon(z, z'') &\equiv \varepsilon_\lambda(q_\parallel, z, z'', \omega) \\ &= \delta(z - z'') - \int \left[\frac{2\pi e^2 \lambda}{q_\parallel} \exp(-q_\parallel |z - z_1|) \right. \\ &\quad \left. + f_{xc\lambda}(z, z_1) \right] \chi_0(q_\parallel, z_1, z', \omega = is) dz_1. \end{aligned} \quad (6)$$

(iv) The resulting interacting response χ_λ was substituted into the exact adiabatic connection–fluctuation-dissipation (ACF/FDT) formula for the exchange-correlation energy of an inhomogeneous electron gas:^{28–30}

$$\begin{aligned} E_c = -\frac{\hbar}{2\pi} \int_0^1 d\lambda \int_0^\infty ds \int d^3r d^3r' \left\{ \frac{e^2}{|\vec{r} - \vec{r}'|} [\chi_\lambda(\vec{r}, \vec{r}', \omega = is) \right. \\ \left. - \chi_0(\vec{r}, \vec{r}', \omega = is)] \right\}. \end{aligned} \quad (7)$$

This result follows by combining the adiabatic connection formula (ACF) with the zero-temperature fluctuation-dissipation theorem (FDT). In Eq. (7), $\chi_\lambda(\vec{r}, \vec{r}', \omega = is)$ is the imaginary-frequency Kubo density-density response function of the whole system, with an additional external potential $V_\lambda(\vec{r})$ added so as to maintain the true ($\lambda=1$) ground-state density $n(\vec{r})$ in the presence of a modified electron-electron interaction $\lambda V_{coul} \equiv \lambda e^2/|\vec{r} - \vec{r}'|$. The $\lambda=0$ response χ_0 is thus the Kohn-Sham density-density response: i.e., it is the response of independent Fermions moving in the groundstate Kohn-Sham potential $V_{KS}(\vec{r})$, the latter being the one-particle potential required to produce the true interacting groundstate density when acting on independent Fermions. In practice the constant-density constraint is easily implemented: we simply use the same KS response from item (ii) above, for all values of λ in Eq. (3) (see also Ref. 24).

In the present geometry, Fourier transformation in the x and y direction converts the ACF/FDT Eq. (7) into

$$E_c/A = -\frac{\hbar}{2\pi} \int_0^1 d\lambda \int_0^\infty dq_\parallel J_c(q_\parallel, \lambda), \quad (8)$$

where $A \rightarrow \infty$ is the surface area and

$$J_c(q_\parallel, \lambda) = \int_0^\infty j_c(q_\parallel, s, \lambda) ds, \quad (9)$$

with

$$\begin{aligned} j_c(q_\parallel, s, \lambda) = 4\pi^2 e^2 \int_{-\infty}^\infty dz dz' \exp(-q_\parallel |z - z'|) [\chi_\lambda(q_\parallel, z, z', is) \\ - \chi_0(q_\parallel, z, z', is)]. \end{aligned} \quad (10)$$

In practical calculations of the correlation energy, it is not necessary to solve explicitly for χ_λ . Equation (10) can alternatively be written as

$$j_c(q_\parallel, s, \lambda) = 4\pi^2 e^2 \int_{-\infty}^\infty dz 2q_\parallel [\delta n_\lambda(z, z) - \delta n_0(z, z)]. \quad (11)$$

Here

$$\begin{aligned} \delta n_\lambda(z_1, z_2) &= \int dz' \chi_\lambda(z_1, z', q_\parallel, is) \frac{\exp(-q_\parallel |z' - z_2|)}{2q_\parallel} \\ &= \int \varepsilon_\lambda^{-1}(q_\parallel, z_1, z'', \omega) \chi_0(z'', z', q_\parallel, is) \\ &\quad \times \frac{\exp(-q_\parallel |z' - z_2|)}{2q_\parallel} dz'' dz' \end{aligned} \quad (12)$$

is the density perturbation at position z_1 induced by a sinusoidally modulated sheet of external charge placed at position z_2 . In practice we solved this by discretizing the space integrations on the same even spatial grid used previously to tabulate χ_0 . We inverted the discretized ε_λ once for each set of values $(q_\parallel, s, \lambda)$ by LU decomposition.

The correlation energy approach described here involves significant numerical computation, and accordingly we applied it to thin jellium slabs rather than thick or semi-infinite ones, in order to minimize the computational cost.

For most of the calculations reported here, the exchange-correlation kernel f_{xc} in Eq. (3) was taken as zero, yielding the pure RPA response. For $r_s=4.00$, however, we also report the response using the “energy optimized local xc kernel” f_{xc}^{enopt} described in Ref. 12. This is local and frequency independent but has the following desirable property: when applied to the uniform electron gas it yields a response that gives the exact correlation energy when put into the adiabatic-connection-fluctuation-dissipation formula (7). Although the inclusion of f_{xc}^{enopt} significantly affected the absolute correlation energy, it had essentially no effect on the “cross” or “interaction” energy between the slabs. See Eq. (14) and also the open circles in Fig. 2(b). Consequently we judged that local xc kernels of this kind would not make a significant difference to the quantities of interest here, and we used only the pure RPA for the rest of our working.

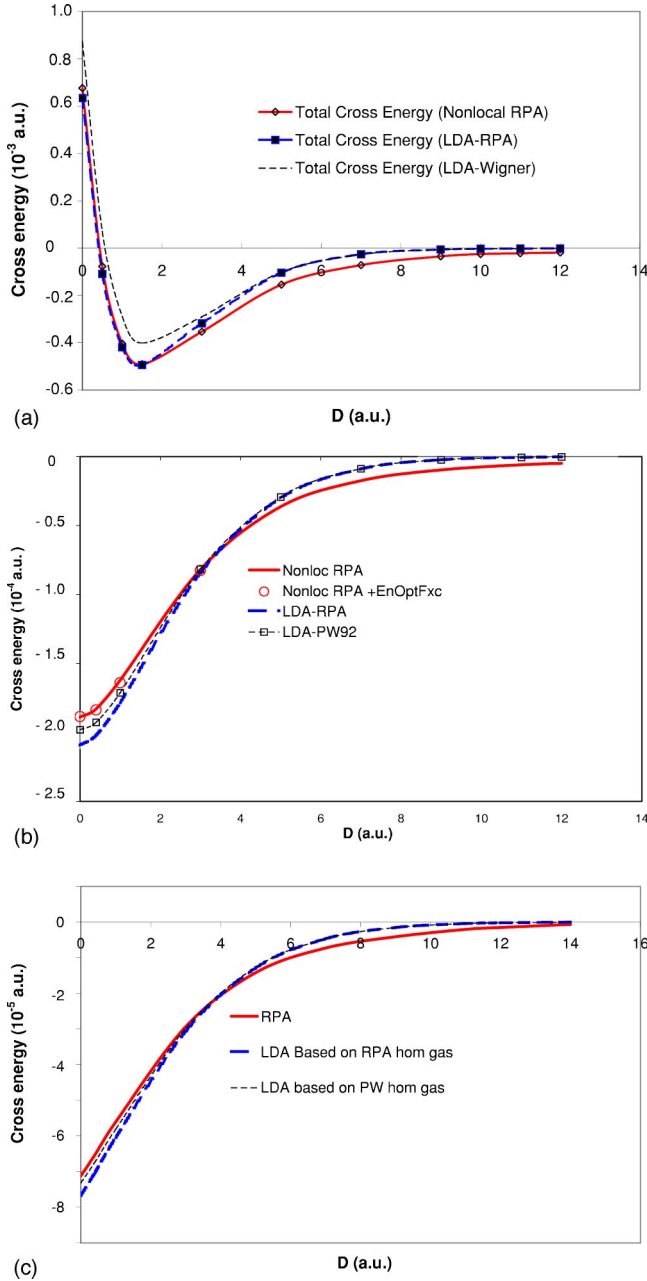


FIG. 2. (Color online) (a) Cross energy E^{cross} [Eq. (14)] versus separation D for slabs of thickness $L=5$ a.u. and with jellium background at the density of Al ($r_s=2.07$). Solid line: nonlocal exchange energy, nonlocal RPA correlation energy. Thick dashed line: LDA using the pure RPA correlation energy of the uniform gas as input. Thin dashed line: LDA using the Wigner correlation energy of the uniform electron gas as input. (b) As for (a), but for $r_s=4.0$ and $L=5.0$ a.u. and with PW92 instead of Wigner uniform-gas correlation employed. Open circles: nonlocal correlation from Eq. (7) with energy-optimized exchange-correlation kernel $f_{xc}^{enopt12}$ included in the RPA-like TDDFT screening Eq. (3). (c) As for (a), but with $r_s=6.0$ and $L=8.0$ a.u.

Similar conclusions had already been reached for $r_s=2.07$ in our earlier work.¹²

The exchange energy of the KS orbitals can be obtained as

$$E_x = -\frac{\hbar}{2\pi} \int_0^1 d\lambda \int d^3r d^3r' \left[\frac{e^2}{|\vec{r}-\vec{r}'|} \left(\int_0^\infty \chi_0(\vec{r}, \vec{r}', \omega = i s) ds - n(\vec{r}) \delta^3(\vec{r}-\vec{r}') \right) \right], \quad (13)$$

where $n(\vec{r})$ is the ground-state electronic density. We found this useful as a test of the method, but for production runs we evaluated E_x directly from overlap integrals using the occupied KS orbitals. The total energy is

$$E = T_s + E_{ext} + E_{NH} + E_x + E_c,$$

where T_s , E_{ext} , and E_{NH} are, respectively, the Kohn-Sham kinetic energy, the interaction between electrons and the positive background, and the “classical” or naive Hartree electron-electron energy.

We define the cross-energy (interaction energy, attraction energy) $E^{cross}(D)$ between the two slabs as the energy per unit area required to bring the slabs from infinite separation to finite separation D :

$$E^{cross}(D) = \frac{1}{A} [E(D) - E(D \rightarrow \infty)]. \quad (14)$$

If the slabs were infinitely thick ($L \rightarrow \infty$) then the magnitude of $E^{cross}(D=0)$ would simply be twice the surface energy,

$$E^{cross}(D=0) = -2\sigma \text{ for } L \rightarrow \infty.$$

Because our slabs are actually very thin, our quantity $E^{cross}(D=0)$ does not exactly give the surface energy. Also note that, by its definition, $E^{cross}(D) \rightarrow 0$ as $D \rightarrow \infty$. It can be shown^{4,11,25} that in the nonretarded RPA, the coupling of two-dimensional plasmons on slabs of finite thickness implies that this decay of the cross energy occurs via a noninteger power law

$$E^{cross}(D) \propto -(\text{const})D^{-5/2} \text{ as } D \rightarrow \infty. \quad (15)$$

It is also known that adding any short-ranged exchange-correlation kernel $f_{xc}(\vec{r}, \vec{r}')$ into the RPA screening (self-consistency) equation does not alter the behavior given in Eq. (15). This is essentially because the asymptotic force is determined by the dispersion of the quasi-two-dimensional plasmons at small wave number, and this in turn is prescribed by a form of the f -sum rule.^{4,19}

III. NUMERICAL CONSIDERATIONS

The convergence parameters affecting our numerical results are as follows:

(i) *Groundstate calculation.* In generating the ground-state density $n(z)$ and KS potential $V_{KS}(z)$ via standard theory (see, e.g., Ref. 19) we solved a one-dimensional Kohn-Sham-Schrodinger equation using a collocation method in position space. The spatial step size dz in the direction perpendicular to the layers was chosen to ensure convergence of n to 10^{-6} of the bulk density, and of V_{KS} to 10^{-6} of the bulk Fermi energy ϵ_F . At $r_s=2.07$ it was found that $dz=0.15$ a.u. was sufficient for this. The KS eigenvalues ϵ_i (for motion perpendicular to the layers) were obtained by shooting and

were converged to $10^{-7}\epsilon_F$. The charge-self-consistency iterations were carried out till convergence was obtained for $n(z)$ and $V_{KS}(z)$ better than that with respect to dz described above. In order to obtain the least error in comparing total energies at different slab separations, we used separations D and a step dz such that the four edges of the jellium backgrounds were sampling points at every separation.

(ii) *Calculation of χ_{KS}* [see Eq. (2)]. Here there was no summation over intermediate states, as the 1D Green function was evaluated by a direct collocation solution of the complex-energy Schrodinger equation. The same range of spatial step sizes was used as for the groundstate Schrodinger solution. The k_x integration in Eq. (2) was converted to a sum using special discrete integration weights adapted to the square-root end singularities of the k_x integrand. The sampled k_x points corresponded to an energy spacing $d\epsilon_x = 0.03\epsilon_F$ or $0.01\epsilon_F$.

(iii) *Inversion of the dielectric matrix (6)*. This was accomplished in position space by discretizing with the same step size dz as described above. Simpson 3/8 integration weights were used, with an interval break at $z=z'$ to account for the discontinuous derivatives $\partial\chi_\lambda/\partial z$ at $z=z'$. Lower-upper (LU) decomposition and backsubstitution were used to invert the resulting matrix ϵ_λ . The dimension of the matrix was up to several hundred for the larger values of slab separation D .

(iv) *Integrating (12)*. The z and z' integrations were performed on the same uniform spatial grid described above, using Simpson 3/8 integration with interval breaks to deal with the derivative discontinuities in the factors of the integrand.

(v) *Imaginary frequency integration* [Eq. (9)]. The integration step for s at $r_s=2.07$ was typically $ds=0.01$ a.u. for $0 < s < 0.2$ a.u., and $ds=0.1$ a.u. for $s > 0.2$ a.u. The maximum imaginary frequency was varied between 2 and 3 a.u.

(vi) *Integration of Eq. (8)*. The Simpson integration grid for q_\parallel was $dq_\parallel \approx 0.05$ a.u. up to $q_\parallel \approx 0.6$ a.u., then $dq_\parallel \approx 0.3$ a.u. up to about 4.2 a.u. An endpoint correction was applied to the integration, based on high- q asymptotics of the uniform electron gas (see Ref. 31).

(vii) λ *integration in Eq. (8)*. This was typically done for $\lambda=0, 1/3, 2/3, 1$. The λ integrand is very smooth.

By varying the above convergence parameters we estimate that the errors in our energy differences E^{cross} are comparable to the vertical size of the symbols in Figs. 2(a) and 2(b).

(viii) *Numerical differentiation of $E(D)$ data to give $F(D)$* . This was done by splining $E(D)$ data. This is probably the largest source of error. By using different forms of spline we could, for example, modify the predicted overestimation of the maximum cohesive force for $r_s=2.07$ between 14% and 18%. The orders of magnitude quoted here are not altered by different splining protocols, however, and our general conclusions are therefore not in doubt.

IV. RESULTS

Figures 2(a)–2(c) plot the cross energy $E^{cross}(D)$ vs D for pairs of slabs distant D and with jellium-background thick-

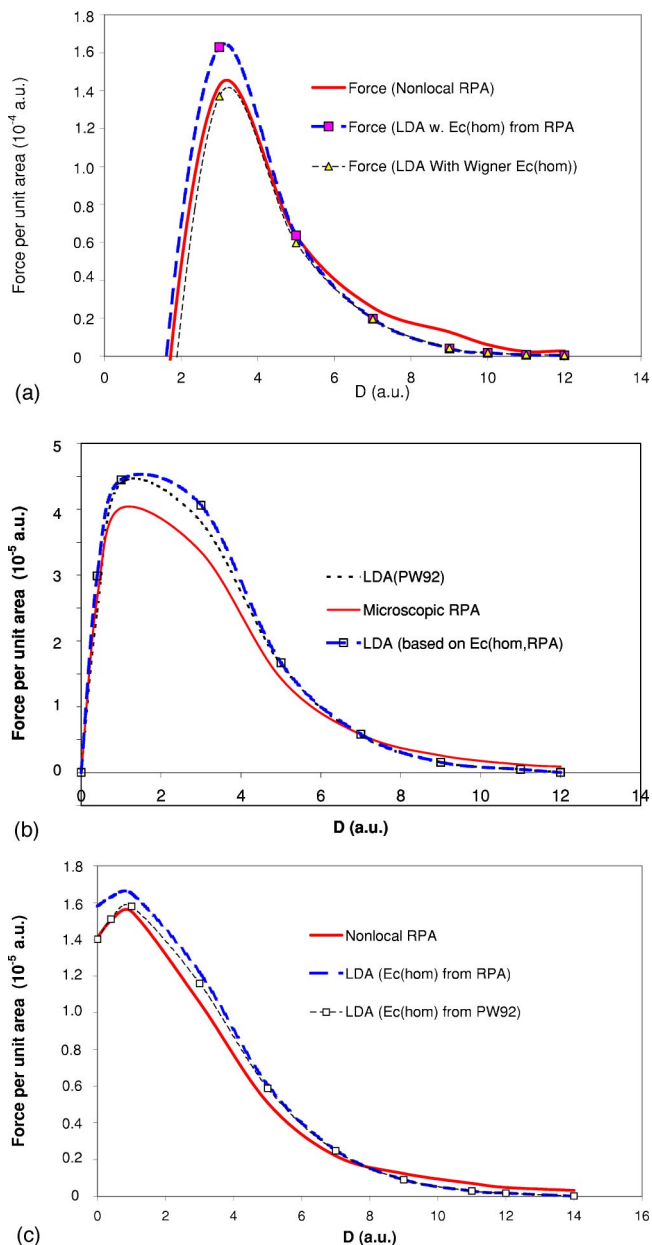


FIG. 3. (Color online) (a): Attractive force per unit area $\partial E^{cross}/\partial D$ for $r_s=2.07$ [for the same slabs as Fig. 2(a)]. (b): Attractive force for $r_s=4.00$, for the same slabs as in Fig. 2(b). (c): Attractive force for $r_s=6.00$, for the same slabs as in Fig. 2(c).

ness $L_1=L_2=L$. Units are atomic units (a_B for D and L , Hartree/ a_B^2 for E^{cross}). Figure 2(a) shows the case $r_s=2.07$, $L=5.00$. Figure 2(b) shows the case $r_s=4.00$, $L=5.00$. Figure 2(c) shows the case $r_s=6.00$, $L=8.00$.

Figures 3(a)–3(c) give the force $F(D)=dE^{cross}/dD$ vs D for the same three systems. Units of F are Hartree/ a_B^3 . In each case results are given using (i) the nonlocal RPA correlation energy from Eq. (7) and the nonlocal exchange energy from Eq. (13) (thick solid line); (ii) local exchange, and local correlation $E_c^{LDA-RPA} = \int n(\vec{r})\epsilon_c^{hom,RPA}(n(\vec{r}))d\vec{r}$ calculated using the pure RPA correlation energy of the uniform gas for the quantity $\epsilon_c^{hom}(n)$ (thick dashed line); (iii) local exchange, and local correlation $E_c^{LDA} = \int n(\vec{r})\epsilon_c^{hom}(n(\vec{r}))d\vec{r}$ calculated using

PW92 correlation energy of the uniform gas for the quantity $\varepsilon_c^{\text{hom}}(n)$ (thin dashed line). (For $r_s=2.07$, the Wigner uniform-gas parametrization was used in place of the PW92 version.)

The pure RPA uniform-gas data was used under (ii) above with the idea that this might better agree with the pure-RPA nonlocal calculations than the conventional LDA energy. This was borne out by the data for the energy near equilibrium at $r_s=2.07$, though the force data was better in the conventional RPA. For higher r_s the regular RPA did slightly better for both energy and force.

V. DISCUSSION

One aspect of the results needs some explanation before we proceed to discuss the energetics of interest. It is well known^{32,33} that the pure jellium model is not in mechanical equilibrium except at $r_s \approx 4$. Specifically, suppose that a large block of jellium metal is cleaved along a plane and the two halves are allowed to separate or overlap until the total energy is minimized, with the positive background remaining rigid within each half. The energy minimum occurs at a separation D_0 that is positive if $r_s < 4$ and negative (i.e., the positive backgrounds would overlap) if $D_0 > 4$. This same behavior is evident in our results, even though we have used very thin slabs of jellium rather than the two infinitely thick layers normally considered in the literature. This behavior is unrepresentative of real metals for which of course the energy of two thick defect-free slabs is minimized at contact so that a perfect combined crystal is produced. More realistic models of metallic cohesion can be created by reintroducing the discrete positive ions into the jellium and treating their effects by pseudopotential perturbation theory.^{14,34–36} Alternatively the simplicity of the jellium metal can be retained, essentially by adding to the electrostatic potential of the positive background a spatially homogeneous additional average potential representing an average of the discrete-ion effects. This can be achieved within two rather similar schemes, the Stabilized Jellium model³² and the Ideal Metal model.³³ We chose instead to use the less realistic standard jellium model because most prior results have been obtained within this model. Accordingly we find that only in the case $r_s=4$ is the minimum total energy achieved at the contact separation $D_0=0$.

A common feature of all the figures is that only the nonlocal RPA-like calculation (thick solid line) gives the required algebraic decay of the energy and force at large separations, correctly corresponding to the van der Waals attraction regime [see Eq. (15)]. As expected, the local-density calculations (dashed lines) have the energy and force vanishing exponentially as the overlap of ground-state densities falls off, thus missing the asymptotic vdW attraction.

Despite this failing at large separations, as is now well known, the LDA gives at least a “fairly good” description of the interaction energy at smaller separations. Here there is significant overlap of electron densities, the total density is not too inhomogeneous, and errors in local exchange and local correlation almost cancel.

Indeed the LDA groundstate energy was once regarded as a very adequate predictor of the energetics of inhomoge-

neous metals. There has subsequently been controversy about the surface energy, however. Some microscopic theories (RPA and RPA+local-kernel approaches^{9,15,16}) strongly support the validity of the LDA for the surface energy of jellium metal, while others [diffusion Monte Carlo³⁸ (DMC)³⁷ and Fermi hypernetted chain^{38,39} (FHNC)] give surface energies different from the LDA predictions. To compound the controversy, there are grounds¹⁵ to suspect that the DMC and FHNC calculations did not correctly extrapolate from finite to infinite slab thickness. Thus the issue of the jellium surface energy is currently unresolved.

The present work does not consider the problem of extrapolation to infinite thickness, but can shed light on some related questions. We have here studied the cross energy (binding energy per unit area) $E^{\text{cross}}(r_s, D, L)$ [see Eq. (14)] as a function of slab separation D , for fixed slab thickness L . We can define a “contact energy”

$$\sigma(r_s, L) = -\frac{1}{2}E^{\text{cross}}(r_s, D=0, L),$$

such that the usual surface energy σ is related to the contact energy for infinitely thick slabs,

$$\sigma(r_s) = \sigma(r_s, L \rightarrow \infty) = -\frac{1}{2}E^{\text{cross}}(r_s, D=0, L \rightarrow \infty).$$

By studying the contact energy and the binding energy curve $E^{\text{cross}}(r_s, D, L)$ as a function of D at a fixed slab thickness L , we have avoided controversy about the extrapolation to infinite thickness. We have used these numbers to generate the attractive force $F(r_s, D, L) \equiv \partial E^{\text{cross}}(r_s, D, L) / \partial D$ and hence the force of maximum attraction $F^{\text{max}}(r_s, L) = \max_D F(r_s, D, L)$ for slab pairs of a given thickness L . The force of maximum attraction is important in general, as it is the force necessary to separate the two samples completely under theoretically ideal planar conditions. It is generally achieved at separations D_{max} at which there is still considerable overlap of electron densities, not in the traditional non-overlapping asymptotic regime $D \gg r_s^{1/2}$ of pure asymptotic van der Waals attraction.

By investigating these quantities we have been able to show that the LDA has some serious problems that are independent of the thickness extrapolation issue. We have found that, because the LDA misses the distant van der Waals attraction, it necessarily has failings at closer slab separations outside the asymptotic vdW regime. In particular, in comparison with results obtained in nonlocal RPA and related correlation theories, the LDA cannot obtain both a good contact energy $\sigma(r_s, L)$ and a good force of maximum attraction $F_{\text{max}}(r_s, L)$ within the same calculation. This will be demonstrated in detail below. The general argument runs as follows. If the contact energy $\int_0^\infty F(r_s, D, L) dD$ is given accurately by the LDA, then since the LDA force F is too small at large separations where there is no overlap, it follows that the LDA force must be too large at smaller separations. This general argument does not indicate the extent of the overestimation of the force, nor whether it occurs at physically interesting separations. In fact, our numbers shown below confirm that the LDA sometimes significantly overestimates

the physically interesting maximum attractive force.

Consider first the slabs of aluminium density [$r_s=2.07$, see Figs. 2(a) and 3(a)]. It is important to note that pure jellium is well-known^{32,33} to have a negative surface energy (mirrored in the negative value of the contact energy that we found for our very thin slabs, and the fact that the minimum energy is reached at a positive slab separation D_0). We find that the LDA-RPA (heavy dotted line, LDA using RPA uniform-gas correlation energy data) fits the nonlocal RPA energy data for the contact energy $E^{cross}(D=0, L=5 \text{ a.u.})$ almost perfectly. It continues to fit $E^{cross}(D, L=5 \text{ a.u.})$ quite well for D values up to the equilibrium point D_0 where E^{cross} has its minimum. For $D > D_0$ the LDA-RPA increasingly underestimates the magnitude of the binding energy. On the other hand, the same LDA-RPA theory does not do particularly well for the force near its maximum, overestimating the maximum attractive force by around 14% [see Fig. 3(a), thick dashed line]. By contrast the LDA-Wigner theory (thin dashed line) gives an excellent value for the maximum force, but it overestimates the magnitude of the (negative) contact energy by about 30% and underestimates the binding energy at equilibrium by about 20%.

Next consider the case $r_s=4$ [Figs. 2(b) and 3(b)]. For this special r_s value, jellium is in equilibrium and correspondingly the minimum energy is achieved with the edges of the jellium backgrounds in contact ($D_0 \approx 0$). We find that the LDA-RPA (heavy dotted line, LDA using RPA uniform-gas correlation energy data) overestimates the nonlocal RPA energy data for the contact energy $E^{cross}(D=0, L=5 \text{ a.u.})$ by about 10%. The LDA with local PW92 xc overestimates the contact energy to by about 5%. Both LDA-RPA and LDA-PW92 overestimate the maximum cohesive force by about 12%.

Finally consider the case $r_s=6$ [Figs. 2(c) and 3(c)]. Here the LDA-RPA overestimates the maximum attractive force by about 6%, and also overestimates the contact energy by about 7%. The LDA-PW92 theory, however, gets both the contact energy and the maximum force about right: an overestimation of the attractive force, by up to about 20%, does however occur at separations D larger than the separation D_{max} where the maximum force occurs.

VI. SUMMARY

We have considered the interaction energy and attractive force as functions of separation D , for pairs of jellium-metal

slabs of various densities but fixed thickness. It is well known that the LDA misses the van der Waals force at large separations where there is negligible overlap of electron clouds. By comparing with microscopic calculations including nonlocal exchange and a nonlocal RPA-type correlation energy, we found that the LDA also makes some errors at closer separations. It tends to overestimate the force of maximum attraction at all densities studied (i.e., for $2.07 \leq r_s \leq 6$), with the strongest effect at low r_s . For low r_s the LDA tends to underestimate the binding energy at equilibrium, with ‘‘LDA-RPA’’ (i.e., LDA using RPA uniform-gas correlation energy) not as bad as regular LDA. For higher r_s (4.0 and 6.0) the LDA calculations tend to bind too much. In a few cases either the force or the binding energy is quite good in one or other version of LDA, but in these cases the other quantity (energy or force respectively) is poorer. Thus in all cases the LDA calculations are unable give accurate predictions of *both* binding energy and maximum attractive force, with the LDA performing worst at high density ($r_s=2.07$). The binding energy is a finite-thickness analog of the surface energy. We have argued that, because the force and energy are related by $E^{cross}(r_s, D, L) = \int_0^\infty F(r_s, D, L) dD$, such failings for overlapped configurations are inevitable in view of the LDA’s underestimation of the van der Waals attractive force at larger separations. The size of these effects at overlapped separations in thin slabs of jellium is around 5–20% at metallic densities, as judged by comparison with microscopic nonlocal RPA calculations. The percentage errors tend to be larger at larger electron densities (smaller r_s). The occurrence of these errors is independent of the issue of finite-thickness extrapolation that has plagued recent work on the surface energy, so we believe we have identified a genuine inadequacy of the LDA.

ACKNOWLEDGMENTS

We thank J. Perdew, A. Rubio, F. Aryasetiawan, P. Garcia-Gonzalez, and J. Jung for useful discussions. This work was supported in part by grants from Griffith University and the Australian Research Council. Computer time was granted by Research Computing Services at Griffith University.

¹P. Hohenberg and W. Kohn, Phys. Rev. **136**, B864 (1964).

²W. Kohn and L. J. Sham, Phys. Rev. **140**, A1133 (1965).

³J. P. Perdew, K. Burke, and M. Ernzerhof, Phys. Rev. Lett. **77**, 3865 (1996).

⁴J. F. Dobson, K. McLennan, A. Rubio, J. Wang, T. Gould, H. M. Le, and B. P. Dinte, Aust. J. Chem. **54**, 513 (2001).

⁵L. A. Girifalco, M. Hodak, and R. S. Lee, Phys. Rev. B **62**, 13 104 (2000).

⁶J.-C. Charlier, X. Gonze, and J.-P. Michenaud, Phys. Rev. B **43**, 4579 (1991).

⁷H. Rydberg, N. Jacobson, P. Hyldegaard, S. I. Simak, B. I.

Lundqvist, and D. C. Langreth, Surf. Sci. **532**, 606 (2003).

⁸H. Rydberg, M. Dion, N. Jacobson, E. Schroder, P. Hyldegaard, S. I. Simak, D. C. Langreth, and B. I. Lundqvist, Phys. Rev. Lett. **91**, 126402 (2003).

⁹Z. Yan *et al.*, Phys. Rev. B **61**, 2595 (2000).

¹⁰J. M. Pitarke and A. G. Eguiluz, Phys. Rev. B **57**, 6329 (1998).

¹¹J. F. Dobson and J. Wang, Phys. Rev. Lett. **82**, 2123 (1999).

¹²J. F. Dobson and J. Wang, Phys. Rev. B **62**, 10 038 (2000).

¹³P. Garcia-Gonzalez and R. W. Godby, Phys. Rev. Lett. **88**, 056406 (2002).

¹⁴N. D. Lang and W. Kohn, Phys. Rev. B **1**, 4555 (1970).

- ¹⁵J. M. Pitarke and J. P. Perdew, Phys. Rev. B **67**, 045101 (2003).
¹⁶S. Kurth and J. P. Perdew, Phys. Rev. B **59**, 10 461 (1999).
¹⁷M. Bostrom and B. E. Sernelius, Phys. Rev. B **61**, 2204 (2000).
¹⁸Z. Yan, J. P. Perdew, and S. Kurth, Phys. Rev. B **61**, 16 430 (2000).
¹⁹J. F. Dobson, Aust. J. Phys. **46**, 391 (1993).
²⁰G. Vignale and W. Kohn, Phys. Rev. Lett. **77**, 2037 (1996).
²¹G. Vignale, C. A. Ullrich, and S. Conti, Phys. Rev. Lett. **79**, 4878 (1997).
²²G. Vignale, C. A. Ullrich, and S. Conti, Phys. Rev. Lett. **79**, 4878 (1997).
²³J. P. Perdew and Y. Wang, Phys. Rev. B **45**, 13 244 (1992).
²⁴J. F. Dobson, J. Wang, and T. Gould, Phys. Rev. B **66**, 081108(R) (2002).
²⁵B. E. Sernelius and P. Björk, Phys. Rev. B **57**, 6592 (1998).
²⁶W. L. Schaich and J. F. Dobson, Phys. Rev. B **49**, 14 700 (1994).
²⁷E. K. U. Gross and W. Kohn, Phys. Rev. Lett. **55**, 2850 (1985).
²⁸D. C. Langreth and J. P. Perdew, Solid State Commun. **17**, 1425 (1975).
²⁹O. Gunnarsson and B. I. Lundqvist, Phys. Rev. B **13**, 4274 (1976).
³⁰J. Harris and A. Griffin, Phys. Rev. B **11**, 3669 (1975).
³¹J. F. Dobson and G. H. Harris, J. Phys. C **21**, 6127 (1987).
³²J. P. Perdew, H. Q. Tran, and E. D. Smith, Phys. Rev. B **42**, 11 627 (1990).
³³H. B. Shore and J. H. Rose, Phys. Rev. Lett. **66**, 2519 (1991).
³⁴J. F. Dobson and J. H. Rose, J. Phys. C **15**, 7429 (1982).
³⁵J. H. Rose and J. F. Dobson, Solid State Commun. **37**, 91 (1981).
³⁶J. Perdew, Prog. Surf. Sci. **48**, 245 (1995).
³⁷P. H. Acioli and D. M. Ceperley, Phys. Rev. B **54**, 17 199 (1996).
³⁸E. Krotschek, W. Kohn, and G.-X. Qian, Phys. Rev. B **32**, 5693 (1985).
³⁹E. Krotscheck and W. Kohn, Phys. Rev. Lett. **57**, 862 (1986).